



Research Article

A case study on the modeling and simulation of UAVs

Osman Kerem KOÇ¹ , Ali SERTKAYA¹ , Alişan GÖNÜL² , Tolga TANER³ ,
Ahmet Selim DALKILIÇ^{1,*} 

¹Department of Mechanical Engineering, Yildiz Technical University, Istanbul 34349, Türkiye

²Department of Mechanical Engineering, Siirt University, Siirt 56100, Türkiye

³Department of Motor Vehicles and Transportation Technology, Aksaray University, Aksaray 68100, Türkiye

ARTICLE INFO

Article history

Received: 07 September 2022

Accepted: 08 August 2017

Keywords:

Flow Analysis; Structural Analysis; Unmanned Aerial Vehicles; Fluent; Design; ANSYS

ABSTRACT

The flow and structure of an application design for un-manned aerial vehicles (UAVs) are examined in this research. We also show an example of modeling and simulation study with the ANSYS Fluent and Mechanical programs. This research reveals the unmanned aerial vehicle's structural and mechanical design, structure configurations, energy-flow and structural analysis, propulsion and firing systems, prototype production and testing, and design flow models. This study aims to complete the unmanned aerial vehicle design by determining its aerodynamic configurations. Due to the complexity of the design, a preliminary preparation for flow analysis is performed with simplified geometry as well as flow analysis. The unmanned aerial vehicle is tested at different velocities by numerical analysis. In addition, different density flow analyses provide predictions about the aerodynamic forces of the UAVs at different heights and temperatures. The thrust results are 4240 g, power became 1711.62 W with 2.48 g/W efficiency, and 12179 [rpm] revolution for 22.2 V voltage and 77.1 A current, respectively. The 5 different analyses are performed in the range of 2.9-12 million elements, and the solution meshes with the lowest number of elements by performing parametric studies with the ANSYS program that gives the most accurate result.

Cite this article as: Koç OK, Sertkaya A, Gönül A, Taner T, Dalkiliç AS, Wongwises S. A case study on the modeling and simulation of UAVs. J Ther Eng 2024;10(1):164–174.

INTRODUCTION

Because of technological advancements in artificial intelligence in recent years, they have enabled unmanned systems to be included in a broad range of application fields, gaining prominence in the defense industry and aviation in particular. The unmanned aerial systems, which

have brought a new dimension to the defense industry sectors of the countries, have caused a revolutionary transformation on the battlefield and in the fight against terrorism. UAVs (unmanned aerial vehicles) are kept at the forefront as unmanned systems in the defense industry. These vehicles, which contain many different models for a wide variety of

*Corresponding author.

*E-mail address: dalkilic@yildiz.edu.tr

This paper was recommended for publication in revised form by Regional Editor Alibakhsh Kasaeian



missions, remove the duty limitations imposed by the human role and play a revolutionary role in wars.

In the current study, the structural and mechanical design, structure configurations, flow, and structural analysis, propulsion and firing systems, and prototype production of the UAVs, as well as a design that can fulfill the determined missions and features in the best way. The UAV model utilized in computational fluid dynamic (CFD) and mechanical analysis is demonstrated in Figure 1. The main parts of the aircraft such as the wing, tail, body, and landing gear are examined in detail. Information about the design details, analysis methods, and other elements of these sections is presented. In addition to these, a firing system design is developed for the aircraft to perform various missions during flight, and it is controlled over MATLAB. An aircraft model on the computer starts to be produced in design. Simulations are carried out by using flow and mechanical modeling with the ANSYS Fluent and ANSYS Mechanical programs, respectively.

It is an aircraft that does not have a pilot and a passenger in unmanned aerial vehicles (UAV), only carries equipment for the purpose (camera, sensors, etc.), has a remote control or automatic control, and performs its mission [1]. In the UAV Systems Road Map document made by the Turkish Undersecretariat of Defense Industry [2], the roles of UAV systems are broken down into five groups: Attack, Target Simulation, Electronic Warfare, Reconnaissance/Surveillance Support, and Special/Specific Missions. There are different classifications of military-type UAVs. Military UAV classification can be in more than one class [3]. Raymer [4] studied aircraft design with a conceptual approach that was widely discussed for aircraft. Koc et al. [5] also presented the study as an aerodynamic analysis and aero package optimization for trucks. Bredberg [6] investigated turbulence models for the wall boundary condition. Sforza [7] researched wing design according to commercial airplane design principles. Johnson [8] researched wing loading, icing and associated aspects of modern transport design. Banal and Ubando [9] investigated the fuzzy programming approach to UAV preliminary sizing in the study. Sforza also [10] emphasized the manned hyper-sonic missions in the atmosphere for their study. Sforza [11]

determined the wing's properties from the engine selection of UAV design. Sirohi [12] studied bioinspired and biomimetic micro flyers for unmanned aerial vehicles. Sforza [13] obtained the landing gear design for the commercial airplane. Coban and Oktay [14] conducted tactical unmanned aerial vehicles, according to the literature. Utilizing this study, the physical properties and the autopilot system structure as well as the optimization method, Fatma et al. [15] revealed some of the latest developments in the application of UAVs in three main areas: transport, road safety, traffic monitoring, and road infrastructure management. Dündar et al. [16] stated that their aim in their work includes the design stages that include the energy consumption of a fixed-wing (FW) vertical take-off and landing (VTOL) unmanned aerial vehicle (UAV), as well as performance analysis. Alzahrani et al. [17] highlighted existing UAV-supported research, such as routing, cellular communications, data collection, and Internet of Things (IoT) networks, as well as disaster management that supports existing facilitating technologies in the study. Deng et al. [18] drew attention to the impact on the ground, which is important for the UAV's take-off and landing modes during flight, with experiments for both hover and forward flight configurations on the UAV. Tan and Katrancı [19] investigated the effects of unmanned aerial vehicles (UAV) on the battlefield by making determinations about the use of more and widening their usage areas in the coming years. According to the literature, the study determined the effects of unmanned aerial vehicles (UAVs) on the battlefield.

A UAV concept design in the mini class with the gun (to shoot) is applied within the electric motor, fixed-wing, and automatic and remote-controlled, capable of reconnaissance, taking off from the runway, surveillance, and attack with this work. Unmanned combat aerial vehicles (UCAV) are systems that contain weapons as a payload and can carry heavy ammunition such as missile systems as well as light ammunition such as hand grenades and light machine guns, according to the class of UCAV. Apart from the fact that these systems are designed more carefully than unarmed UAVs, the weapon systems cause effects that disrupt the movement in the air, apart from creating an additional load for the UAV. Therefore, necessary analyses should be made for ammunition. Mini UCAVs are light unmanned aerial vehicles weighing 2-20 kg, and although they are generally used for reconnaissance and observation as UAVs, they are armed for simpler armed missions. These UCAVs have two different classes fixed-wing and rotary-wing. Rotary-wing ones can use weapons such as machine guns and bombs, while fixed-wing-type ones are used only for bomb-throwing. These unmanned aerial vehicles, produced for reconnaissance and observation purposes, are armed with additional equipment and sent on some missions, but their main purpose is not armed use. Preliminary design parameters should be determined to produce of a fixed-wing UCAV.

In this study, conceptual design is created by paying close attention to the factors to be considered in UAV design. Mechanical and flow analyses have been employed to

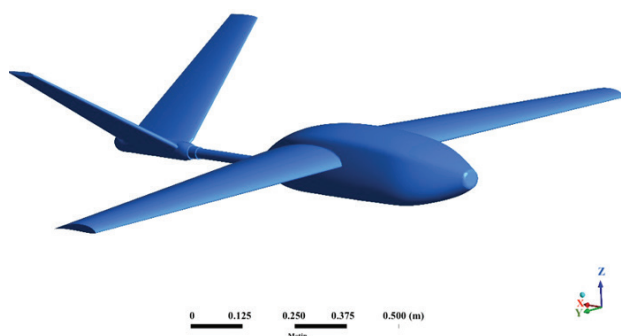


Figure 1. The UAV model used in the analysis.

determine the dimensions of the unmanned aerial vehicle's wings, tail, body, and landing gear. The aerodynamic behavior of the related UAV design is evaluated at various altitudes. In addition, mechanical analyses of the UAV's fuselage-engine and landing gear-fuselage connections are performed. As a consequence of the analyses, the detailed design of the mini unmanned aerial vehicle has been completed as part of the current research.

THEORY

Aerodynamics is the science that studies the forces exerted by the air on an object. Mass effects of air occur because of the movement of air or objects on the object. In in-flight aerodynamics, the air affecting the aircraft during flight is examined, and calculations and analyses are made. Air vehicles are exposed to more aerodynamic effects than land and sea vehicles, and many forces occur that affect the movement of the aircraft. The aerodynamic forces that UAVs are exposed to are divided into four categories. These are carrying, lifting, dragging, and thrust forces [4]. Aerodynamic forces and moments, Mach, and Reynolds numbers can be determined for UAV design. drag force with transport and the resulting moment value can be calculated with the defined equations [4]. Lift

Force (F_L), Drag Force (F_D), and Moment (M) equations are presented from Eq. (1) to Eq. (3) respectively, as follows:

$$F_L = \frac{1}{2} \rho_{\infty} V_{\infty}^2 S C_L \quad (1)$$

$$F_D = \frac{1}{2} \rho_{\infty} V_{\infty}^2 S C_D \quad (2)$$

$$M = \frac{1}{2} \rho_{\infty} V_{\infty}^2 S \bar{c} C_M \quad (3)$$

Aerodynamic coefficients depend on the angle of attack, geometry (profile geometry, wing geometry, aircraft configuration, wet area, etc.), Reynolds number, and Mach number. In this study, the coefficients were calculated for wing and tail selection.

The Reynolds number is a dimensionless number defined as the ratio of the inertial forces of a fluid to the viscosity forces. The value of the Reynolds number allows comment on the flow regime. To determine the Reynolds number for the wing, it is necessary to calculate the coefficients depending on the flow formed on the surface. The calculation of the Reynolds number depends on the fluid's velocity, density, hydraulic diameter, and dynamic (or kinematic) viscosity [20]. In this study, coefficients were obtained by performing analyses depending on the Reynolds number (Re) that is given in Eq. (4) as follows:

$$Re = \frac{\rho V \bar{c}}{\mu} \quad (4)$$

The Reynolds number and values are given as follows; Air density (ρ) 225 kg/m³, velocity (V) 15 m/s, average center length (\bar{c}) 0.262 m, dynamic viscosity (μ) 0.0000179 kg/(m.s), and Re 269,092.27 were employed in the calculations.

The Mach number (Ma) is defined as the ratio of the velocity of a moving mass to the velocity of sound in its environment. The flight is named according to the value of the Ma . If the Ma is less than 1 subsonic and greater than 1, it is considered supersonic velocity [6]. Since the design UCAV flies at an altitude of 1000 meters at a velocity of 15 m/s, the Ma is determined to be 0.045, taking the ratio of sound and UCAV velocity. This value is used in the calculations for the UCAV, which would fly at subsonic velocities since the Ma is calculated to be much smaller than 1.

RESULTS AND DISCUSSION

The flow analysis and boundary conditions are specified in this section. The design of the unmanned aerial vehicle is completed by determining its aerodynamic configurations. Due to the complexity of the design, its geometry is simplified by preparing for flow analysis. Flow analyses are carried out in the ANSYS Fluent program. The flow analyses are compared with the CFD analysis results with the specified configuration. Thus, it could be determined whether the system will work correctly or not.

The flow lines that may cause lift, drag force, and turbulence were researched using CFD analysis. By checking whether the lift and drag forces are sufficient, it is examined whether the lifting force could meet the vehicle's weight at cruising velocity. Drag force is kept to a minimum at specified velocities. In the CFD analysis, the aerodynamic forces of the UAV at different heights and temperatures are determined by testing the UAV at different velocities as well as flow analysis at a different densities. In the CFD analysis, the number and quality of mesh elements are also clarified by referring to the accuracy analysis of the solution mesh. The mesh independence analysis is performed with different mesh element numbers. Apart from the optimum number of elements determined independently of the mesh, accurate results are achieved in

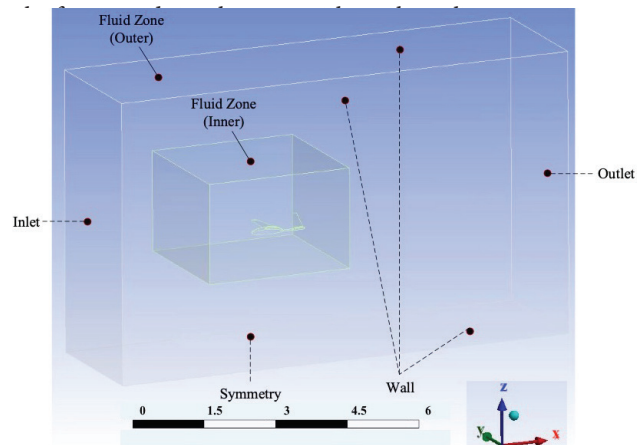


Figure 2. The boundary conditions and fluid zones for CFD analysis.

Figure 2 illustrates boundary conditions in the fluid domain. While the inlet boundary condition is constant velocity, the outlet boundary condition is atmospheric pressure. To facilitate the number of meshes and resolution, the flow dominated approaches taken by considering half of the UAV. The symmetry boundary condition is applied to the relevant surfaces. A new zone has been created to better examine the flow in regions close to the UAV within the streaming domain. Meshes are engaged in this zone with smaller meshes than in the outer fluid zone. The wall boundary condition is defined for UAV surfaces and other surfaces. While the distance between the input and UAV is as 5 of the chord length, the distance between the output and the UAV is 10 times the chord length. Similarly, the distance between the other walls and the UAV is taken 5 times the chord length. The surface area obtained because of the design affects the lift and drag forces of the drone. Some parameters affecting the lift force and drag force are pre-sented in Table 1.

To facilitate the solution, the mesh is created with the sweep method in uncomplicated geometries, as shown in Figure 3 [5]. Although hexagonal mesh is tried to be created in sections where complex geometries occur, tetragonal mesh structure is applied as an alternative and is shown in Figure 3b). This situation causes the number of elements to increase and the analysis to be prolonged. In the boundary layer behaviors, inflation layers in subsonic aerodynamic flow analysis are applied (Figure 3c).

In CFD analysis, the solution mesh is of great importance regarding the accuracy of the analysis. Thanks to the optimum number of elements determined independently of the mesh, it has provided accurate results in the fastest and simplest way with mesh quality [21]. With this parametric study, a solution mesh with the least number of elements, which can give the most accurate result, was determined by applying four different analyses in the range of 2.9-12 million. It is observed to converge in the range of 6-12 million mesh elements. The analysis with 6,031,055 elements is determined as the optimum solution mesh. F_L and F_D changes are demonstrated according to the number of meshes created for mesh independence analysis in Figures 4 and 5, respectively.

Table 1. The lift and drag forces of the UAVs parameters

	Lift force	Drag force
Parameters	15	15
V (m/s)	0.471	1.07
ρ_{ho} (kg/m ³)	1.07	0.184
Area (m ²)		2%
Turbulence intensity (%)	2%	
Temperature (K)	288	288

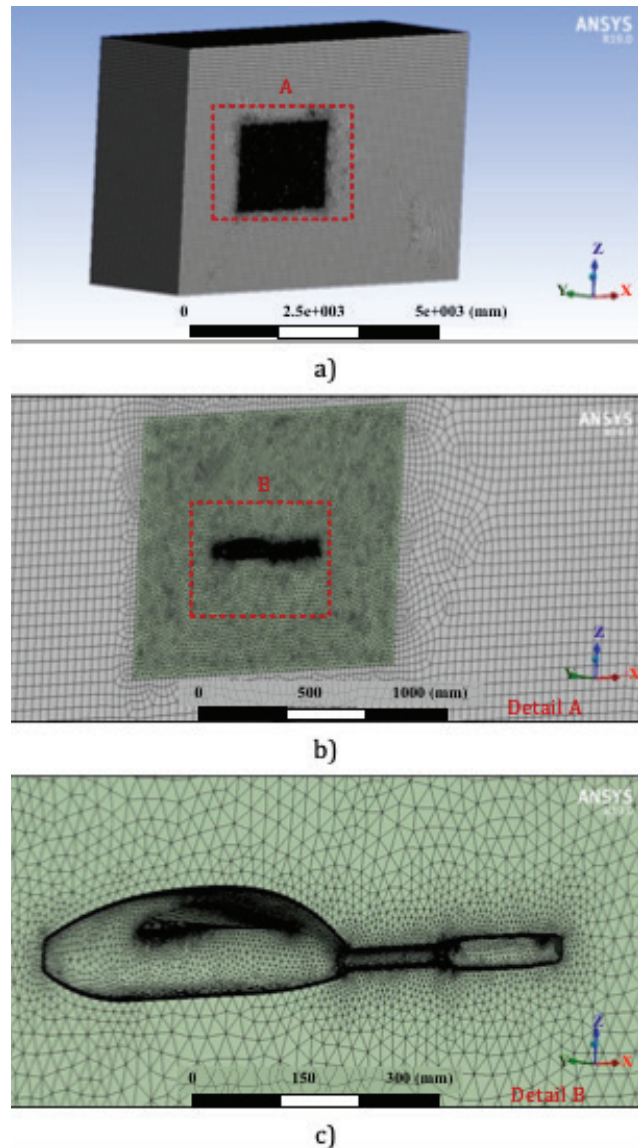


Figure 3. Mesh structure (a) General view, (b) Inner zone detail, (c) Mesh structure on UAV's wall detail.

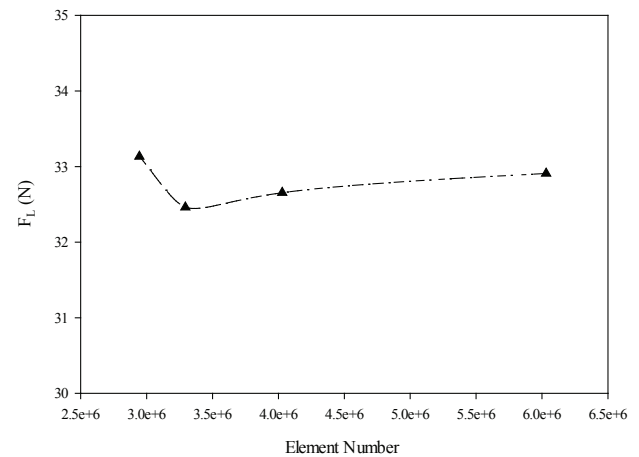


Figure 4. Number of elements-lift force curve (Independency of mesh).

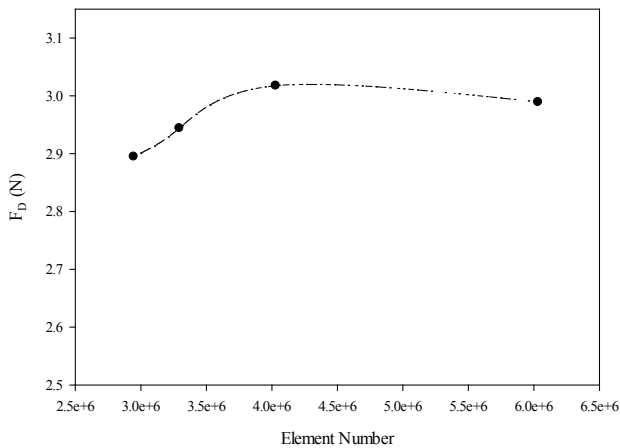


Figure 5. Number of elements-drag force curve (Independency of mesh).

Table 2. The method mesh and Sweep-Tetragonal forms

	Method	Sweep-Tetragonal
Mesh	Elements number	6,031,055
	Skewness (Average- maximum)	0.22635-0.9259
	Aspect ratio (Average-maximum)	4.3072-781.71
	Orthogonal quality (Average)	0.72232

The mesh properties used in the analysis are listed in Table 2. In describing the mesh size for a particular flow pattern, the dimensionless value y^+ is commonly employed.

In the ANSYS Fluent Setup section, $k-\omega$ SST is chosen as the flow turbulence model. In determining the appropriate

size of the cells near the field walls in turbulence modeling, the turbulence model laws have restrictions on the y^+ value in the wall [6]. In Figure 6, it is tried to keep the y^+ value below 2 to increase the accuracy of the analysis in the $k-\omega$ SST model. The number of inflation layers is determined as 15, the growth ratio is 1.2, and the first-layer thickness is 0.1 mm. The setup model is created as Pressure Based, Air, $k-\omega$ -SST, Production Limiter (On), and Curvature Correction (On). Due to the curvature correction, a production lim-iter has been activated to obtain more precise results with the help of solution methods.

Aerodynamic force analysis at different velocities is also analyzed in this way. The aerodynamic analysis is performed at different velocities to examine the aerodynamic behavior and the resulting forces. It is noticed that the cruise velocity is determined, as is whether the thrust will meet the drag force. In Figure 7, the aerodynamic flow lines formed on the unmanned aerial vehicle are examined. The streamlines reach their highest velocities on the main airfoil, causing a pressure drop. Under the wing, the slowing flow causes high pressure and lift force. It is very important for flight dynamics that the lines of the flow are continuous and balanced. The pressure drop caused by turbulence may occur behind the UAV, increasing the drag force but causing instability. For the continuity of the flow, it is of great importance that the flow surface is produced smoothly and precisely.

In Figures 8 and 9, the analysis results are determined between the ranges of 10 and 20 m/s. Varying lift and drag forces are seen depending on the velocity. The density is determined by the average weather condition, which varies depending on the time and place of the flight. The cruising velocity is determined as 16.5 m/s in the equilibrium

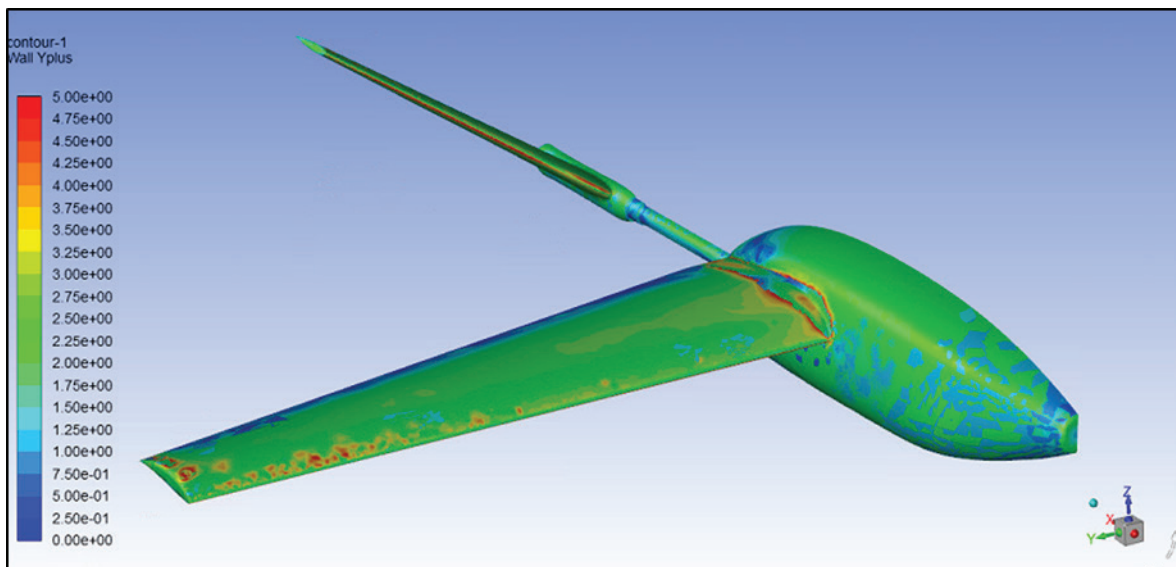


Figure 6. The accuracy of the analysis in the $k-\omega$ SST model (UAV y^+ contour with ANSYS Fluent analysis).

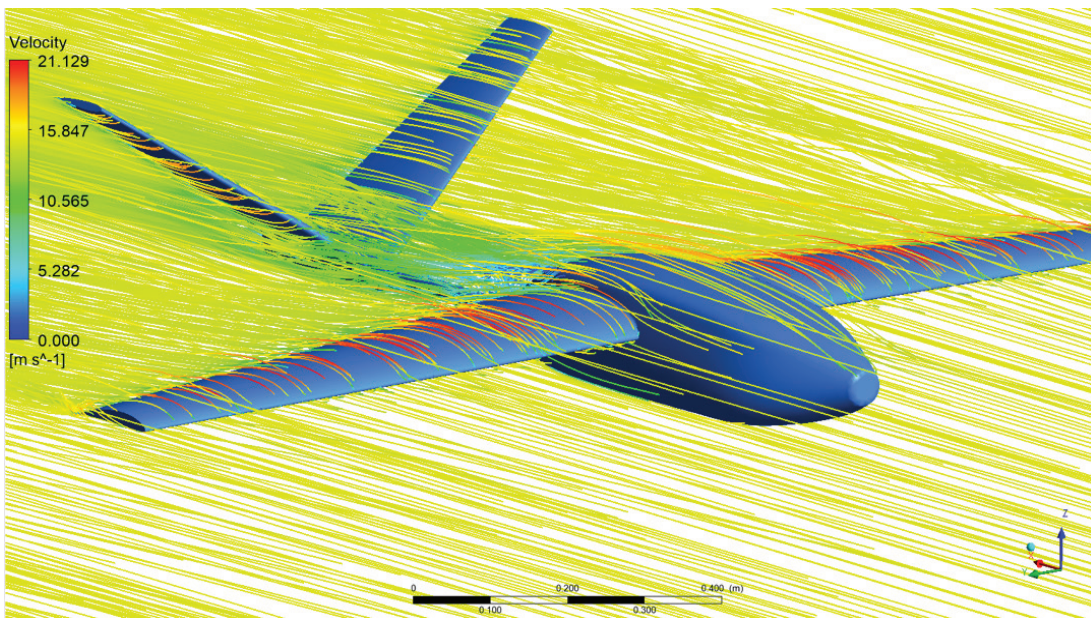


Figure 7. UAV aerodynamic flow lines.

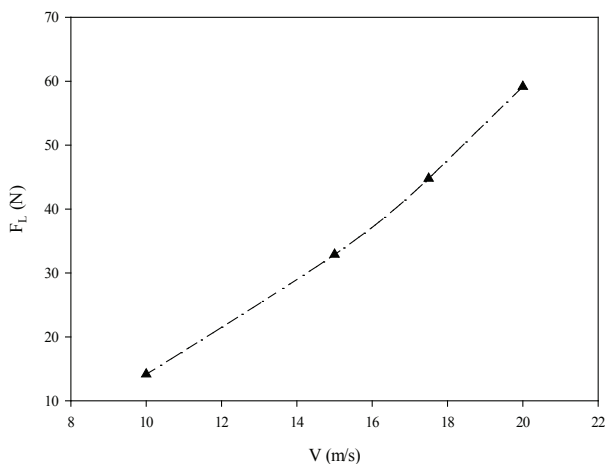


Figure 8. Velocity and lift force curve for 1.07 kg/m³.

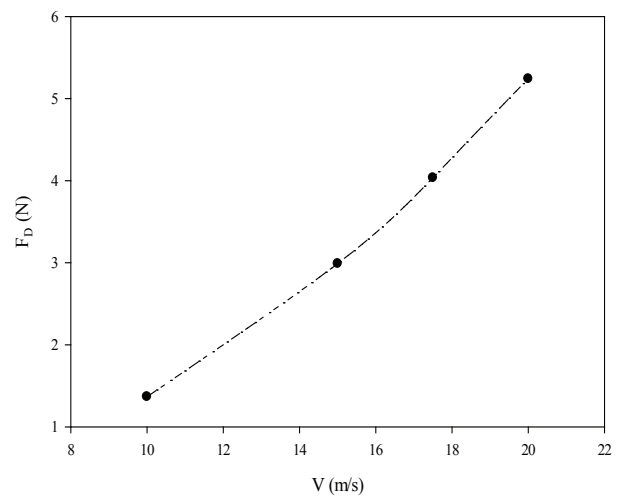


Figure 9. Velocity and drag force curve for 1.07 kg/m³.

condition without the attack angle in the air condition of 1.07 kg/m³ density.

At lower velocities, the angle of attack is increased to provide sufficient lift. It has been determined that it can carry up to 6 kg at velocities up to 20 m/s (UAV + payload). The pressure contour obtained because of the analysis is illustrated in Figure 10.

The pressure reaches its highest levels in regions where the flow velocity approaches 0. Thus, the high pressure generates at the front surface increases the drag force. Besides, the engine thrust must overcome the drag force and acceleration resistance. It provides the necessary lifting force for the UAV by reaching sufficient velocities. It is noticed that the drag force is at the expected level in this

analysis. Today’s unmanned aerial vehicles undertake different missions for reconnaissance, surveillance, and attack purposes. These tasks are performed in different weather conditions. Density varies depending on climatic and altitude differences [22]. In this investigation, aerodynamic flow analyses have been conducted for varying densities.

Figures 11 and 12 depict the lift force and drag force curves under variable density conditions at a 15 m/s velocity assumption. Because of this investigation, the results of the lift and drag analyses are presented. The outcomes of the studies are determined as analysis results and aerodynamic coefficients at 15 m/s velocities (assumption for the analysis) and are listed in Table 3.

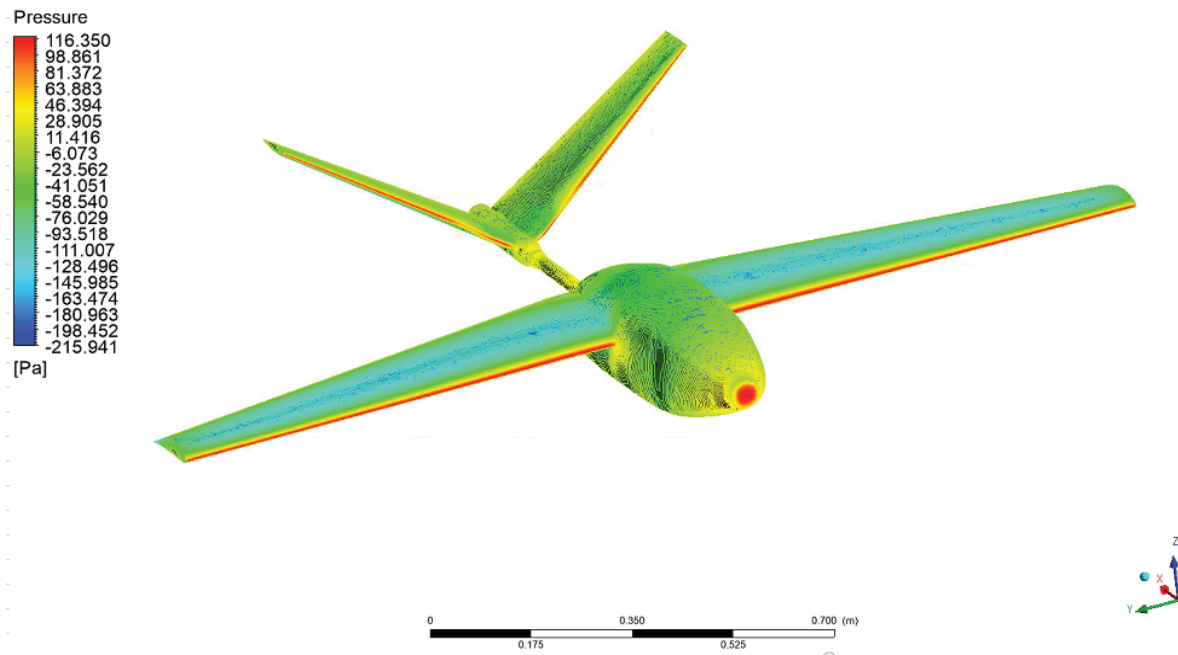


Figure 10. UAV pressure contour.

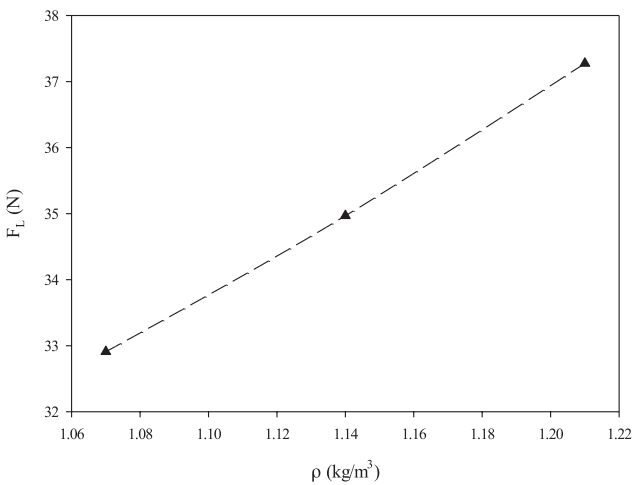


Figure 11. Density and lift force curve.

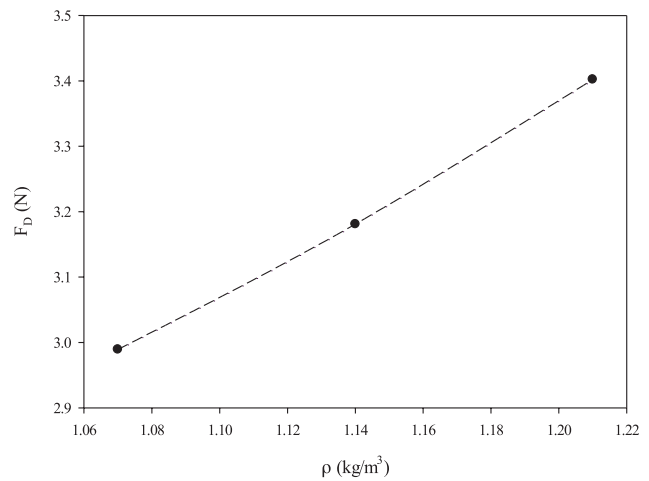


Figure 12. Density and drag force curve.

Table 3. The results of the study for the lift and drag forces of the UAVs parameters.

Parameters	Lift force (Buoyancy)	Drag force
V (m/s)	15	15
ρ (kg/m ³)	1.07	1.07
Area (m ²)	0.471	0.184
Turbulence intensity (%)	2%	2%
T (K)	288	288
F (N)	32.91	3.18
Coefficient (-)	0.580	0.143

Structural analysis based on CFD analysis presents a continuation axis for the study of UAVs. In the structural analysis of the UAV, the structural strengths of critical elements are measured for the riskiest situations seen during flight. During the take-off and landing of the aircraft, dynamic loads varying in time according to the engine operating cycle have been tested. The strength values at the fasteners and points transferred to the aircraft have been examined. In this study, the structural analysis of front body-engine connection and landing gear-body connections has been applied. Front body-engine connections structural analysis is applied as follows; On the front body of the electric

motor, the 29.9 kg/m³ density Styrofoam body and the motor mass-produced an average thrust, and 45 N of inertia forces were dealt with. The mesh structure of the aircraft body, the number of nodes and elements, the total deformation amount of the front fuselage, and the safety factor are given in Figure 13.

The number of nodes is found to be 370,415; the number of elements was 207,000, the maximum displacement in the body is 0.267 mm and the safety factor is 0.64. The displacement values in the aircraft body are obtained by forcing a thrust force of 45 N at an angle of 3°. With the structural analysis of the load zones of the landing gear

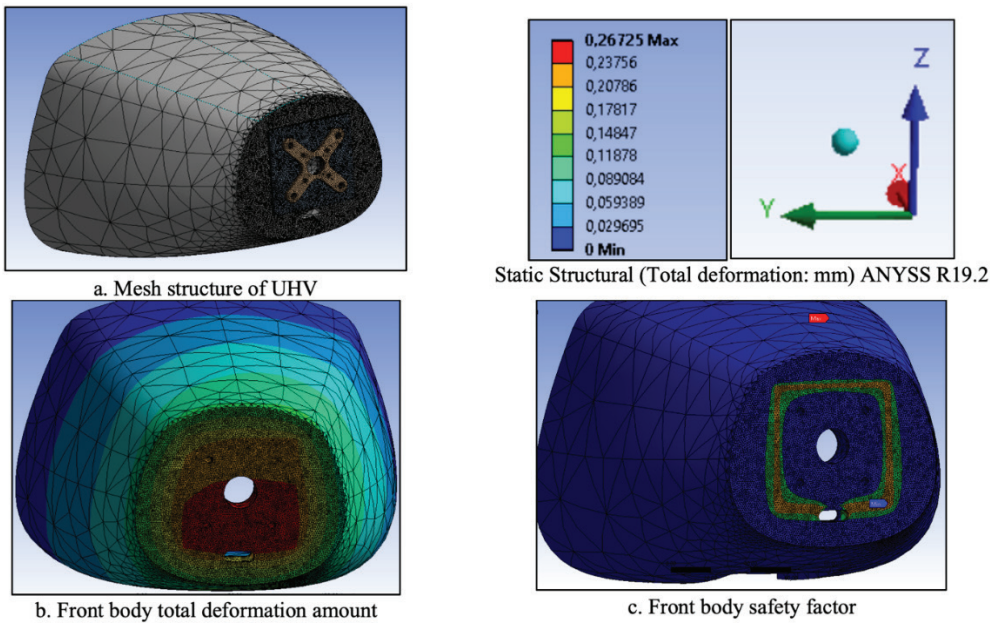


Figure 13. The mesh structure of UAV and body state.

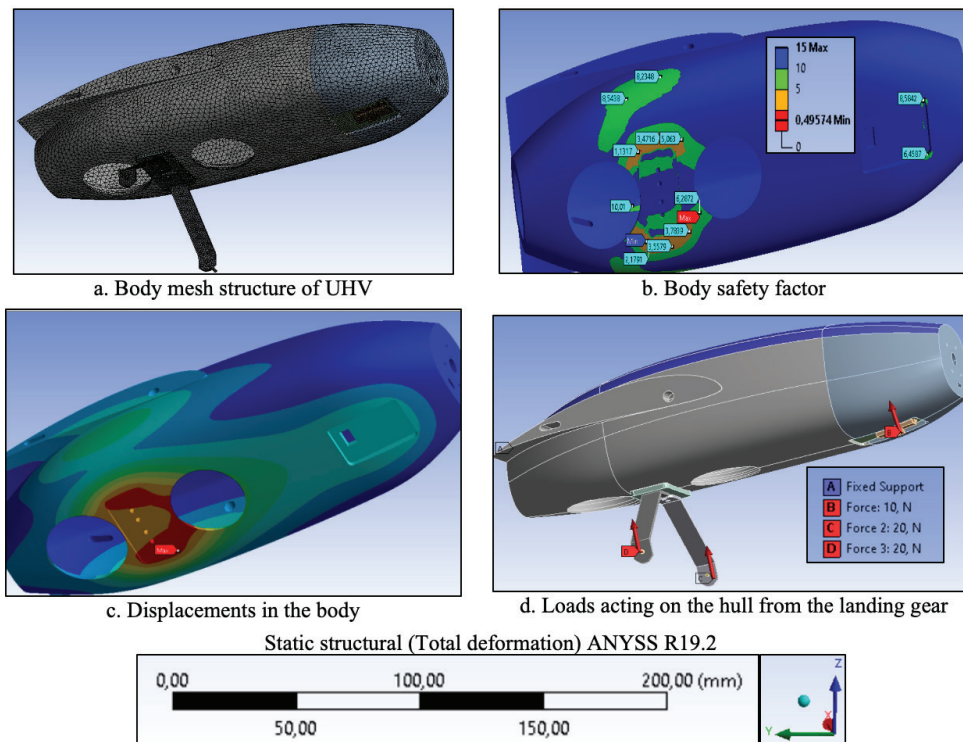


Figure 14. Body mesh structure and technical values.

combined with the fuselage, the load distribution of the front and rear landing gears to the fuselage is calculated as 20% for the front landing gear and 40% for each rear landing gear, respectively.

In Figure 14, the force generated for a body mass of 3.9 kg is found to be 38.259 N. The dynamic load due to the inertia and acceleration during the landing corresponds to 45 N. Thus, a force of 10 N on the front landing gear and 20 N on the rear landing gear is affected. The mesh structure formed in the body material, the number of nodes and elements, the displacement, and the safety coefficient in the body are presented in Figure 14. The knot number of the mesh structure is 256,267, the number of elements is 158,184; the maximum displacement in the body is 1.266 mm; and the material safety factor is 0.495.

In Figure 15, the tail and wing areas of the unmanned aerial vehicle are produced by the hot wire cutting method. XPS Styrofoam foam material is used in wings and tail material. Photographs of the design are presented in Figure 15a. A hot wire cutting machine to produce wing and tail structures and a wire machine, as presented in the

figure, are designed and produced to give profile shapes. The power source of the wire-cutting machine is 12 V, and its current rating is 10 A. In Figure 15b, the wing profile, is determined as the tail profile as NACA 0012. These profiles are glued to wood for wing production and then cut with laser cutting, and the geometry of the profile is transferred to the wood to be used as an auxiliary element in production. Wing and tail geometries made of XPS Styrofoam are designed in Figure 15b.

The test has been performed under various loads on the propulsion engine within the scope of the study. The supplier of the electric motor using a brushless electric motor published Sunnysky as thrust provider X3530. A 12x8-propeller thrust with a test 6S battery (22V) is to be produced at approximately the maximum thrust force of 4240 g. According to the results of the SunnySky X3530 brushless electric motor impulse test, the voltage, power, current, impulse, and efficiency are determined in Table 4. With the operation of the brushless electric motor, the impulse value that affected the sensitive balance is presented in Table 4. The effect of the assembly on the precision balance with the engine not running is



(a) Hot wire cutting machine



(b) Wing and tail geometries made of XPS Styrofoam 1



(c) Impulse test equipment



(d) Ready to flight UAV

Figure 15. Wing and tail profiles production.

Table 4. The catalog data of the SunnySky X3530 brushless electric motor impulse test, the voltage, power, current, impulse, and efficiency

Prop [inch]	Voltage [V]	Current [A]	Thrust [g]	Power [W]	Efficiency [g/W]	Revolution [rpm]	Load temperature in 100% throttle
APC 12x8		3.1	500	68.82	7.27	4154	115°C-50 s
	22.2	19.9	2000	441.78	4.53	8119	
		77.1	4240	1711.62	2.48	12179	
		2.8	500	70	7.14	4230	
	25.0	22.0	2250	550	4.09	8640	
		96.1	5180	2402.5	2.16	13260	

measured as a mass of 594 g. The electric motor is operated with various currents and compared with the data provided by the supplier. While the supplied electric motor, which has a mass of 4240 g, gives the amount of thrust produced at full power, it is noticed that the measured value in the precision balance is 4200 g. The thrust test setup is as shown in Figure 15c. It is thought that the difference might be due to friction in the installed setup. The thrust value remains within acceptable limits, and the test is successfully completed.

CONCLUSION

According to the detailed design and analysis of the mini-UCAV, the wing, tail, body, landing gear, shooting systems, and engine have been examined. Parameters are determined and the decision method is mentioned. These values are supported by analysis by paying attention to the values found and suggested in the literature. Since the detailed design throughout the study includes a system design, it is determined that the information and values in each section affect other designs. This work required optimization work. Therefore, it led to recalculation and analysis.

- The wing design is the first UCAV section to be examined. While designing and analyzing the wing, it is started by making certain acceptances as it is the first design part. These assumptions are changed later in the study, and optimization is achieved again.
- While designing and analyzing the tail, it was determined that the tail design was based on the wing design. It has been noticed that the wing design and center of gravity directly affect the tail design. The design is completed by examining the important design requirements mentioned in the literature for a tail design.
- In the body design, the most suitable aerodynamic shape is made by taking manufacturability into consideration. In the landing gear design, control and analysis studies were carried out to ensure that the aircraft could move safely.

- This study aimed to carry out an appropriate aerodynamic and structural design to perform the current gun release task in the design of the UCAV’s firing system.
- For the propulsion system, the most suitable propulsion system is determined with the help of the values obtained according to the analyses. The final design was obtained by combining each of the examined UCAV sections, and the detailed design emerged.
- According to the detailed design determined, wing and tail production is started depending on the analyses’ results. The load test of the produced wing is carried out and the thrust value produced by the engine is measured. These results are found to be compatible with the literature.
- The flight is successfully completed after all production processes for the UAV.

NOMENCLATURE

- \bar{c} Average center length, m
- C Coefficient
- F Force, N
- g Gravity acceleration, m/s²
- M Moment, N.m
- Re Reynolds number
- S Area, m²
- T Temperature, K
- V Air velocity, m/s

Greek symbols

- μ Dynamic viscosity, kg/m.s
- ρ Air density, m³/kg

Subscripts

- D Drag
- L Lift
- ∞ Free stream

Acronyms

- UAV Unmanned Aerial Vehicle
- UCAV Unmanned combat aerial vehicle

CFD	Computational Fluid Dynamic
FW	Fixed-Wing
IoT	Internet of Things
RANS	Reynolds-averaged Navier-Stokes
XPS	Extruded Polystyrene
VTOL	Vertical Take-off and Landing

ACKNOWLEDGMENT

This study was carried out as the flow analysis of the unmanned aerial vehicle, which was supported by the 2020 TUBITAK (The Scientific and Technological Research Council of Turkey) Unmanned Aerial Vehicle Competition (Project Funding Number 548110 and Date 15-20 September 2020) and was based on the altitude of Gaziantep.

AUTHORSHIP CONTRIBUTIONS

Authors equally contributed to this work.

DATA AVAILABILITY STATEMENT

The authors confirm that the data that supports the findings of this study are available within the article. Raw data that support the finding of this study are available from the corresponding author, upon reasonable request.

CONFLICT OF INTEREST

The author declared no potential conflicts of interest with respect to the research, authorship, and/or publication of this article.

ETHICS

There are no ethical issues with the publication of this manuscript.

REFERENCES

- [1] Can N, Kahveci M. Unmanned aerial vehicles: History, definition, legal status in Turkey and the World. *Selcuk Univ J Eng Sci Tech* 2017;5:511–535. [\[CrossRef\]](#)
- [2] Presidency of Defence Industries, Presidency of the Republic of Turkey. Turkey unmanned aircraft systems roadmap (2011-2030). 2011 [in Turkish]. Available from: www.ssb.gov.tr. Access date: 21/10/2020.
- [3] Akyürek S, Yılmaz MA, Taşkiran M. Unmanned aerial vehicles file: Revolutionary transformation in the battlefield and combating terrorism. Wise Men Center for Strategic Studies (Bilgesam), 2012 [in Turkish].
- [4] Raymer D. Aircraft design: A conceptual approach. Sixth Edition. AIAA Education Series, American Institute of Aeronautics and Astronautics Inc., Ohio, 2018. [\[CrossRef\]](#)
- [5] Koç OK, Kırklaroğlu M, Dalkılıç AS, Gönül A, Deniz Y. Aerodynamic analysis and aero package optimization in trucks. Istanbul, ICAME, 2019.
- [6] Bredberg J. On the wall boundary condition for turbulence models. Internal Report 00/4, Chalmers University of Technology, Göteborg, 2000.
- [7] Sforza FM. Chapter 5 - Wing Design. *Commercial Airplane Design Principles*. 2014;119–212. Elsevier. [\[CrossRef\]](#)
- [8] Johnson CL. Wing loading, icing and associated aspects of modern transport design. *J The Aeronaut Sci*. 1940;8:43–54. [\[CrossRef\]](#)
- [9] Banal LF, Ubando AT. Fuzzy programming approach to UAV preliminary sizing. 8th IEEE Int Conf (HNICEM), Cebu City, 2015. [\[CrossRef\]](#)
- [10] Sforza FM. Chapter 4 - Manned Hypersonic Missions in the Atmosphere. *Manned Spacecraft Design Principles*. 2016;59–74. Elsevier. [\[CrossRef\]](#)
- [11] Sforza FM. Chapter 4 - Engine Selection. *Commercial Airplane Design Principles*. 2014;81–118. Elsevier. [\[CrossRef\]](#)
- [12] Sirohi J. Chapter 5 - Bioinspired and Biomimetic Microflyers. *Engineered Biomimicry*. 2013;107–138. Elsevier. [\[CrossRef\]](#)
- [13] Sforza FM. Chapter 7 - Landing Gear Design. *Commercial Airplane Design Principles*. 2014;251–300. Elsevier. [\[CrossRef\]](#)
- [14] Coban S, Oktay T. A review of tactical unmanned aerial vehicle design studies. *The Eurasia Proceedings of Science, Technology, Engineering & Mathematics (EPSTEM)*. 2017;1:30–35.
- [15] Outay F, Mengash HA, Adnan M. Applications of unmanned aerial vehicle (UAV) in road safety, traffic and highway infrastructure management: Recent advances and challenges. *Transp Res Part A*. 2020;141:116–129. [\[CrossRef\]](#)
- [16] Dündar Ö, Bilici M, Ünler T. Design and performance analyses of a fixed wing battery VTOL UAV. *Eng Sci Technol Int J*. 2020;23:1182–1193. [\[CrossRef\]](#)
- [17] Alzahrani B, Oubbati OS, Barnawi A, Atiquzzaman M, Alghazzawi D. UAV assistance paradigm: State-of-the-art in applications and challenges. *J Network Comput Appl*. 2020;166:102706. [\[CrossRef\]](#)
- [18] Deng S, Wang S, Zhang Z. Aerodynamic performance assessment of a ducted fan UAV for VTOL applications. *Aerosp Sci Technol*. 2020;103:105895. [\[CrossRef\]](#)
- [19] Tansü YE, Katrancı S. The use of unmanned aircraft in combat-defense system and the effect of unmanned aircraft on Turkish Armed Forces. *Int J Soc Humanit Adm Sci*. 2020;6:340–345.
- [20] Çengel YA, Cimbala JM. Fluid mechanics, fundamentals and applications. McGraw-Hill Higher Education, Boston, 2014.
- [21] Mesh Independence Study. Available from: www.featips.com. Access date: 20/12/2019.
- [22] Çengel YA, Boles MA. Thermodynamics: an Engineering Approach. McGraw Hill, New York, 2011.